

Nuclear magnetic resonance spectrometer with a frequency range extended below the megahertz region

R. Sitnikov, I. Furó,^{a)} and U. Henriksson

Division of Physical Chemistry, Department of Chemistry, Royal Institute of Technology, Stockholm, SE-10044, Sweden

F. Tóth

Research Institute for Solid State Physics and Optics, MTA KFKI, Budapest, H-1525, Hungary

(Received 8 September 1999; accepted for publication 20 October 1999)

A conventional nuclear magnetic resonance (NMR) spectrometer with an original low-frequency limit of 2 MHz and equipped with an electromagnet is rebuilt to allow performing NMR experiments at resonance frequencies down to 100 kHz. The instrument is intended for accurate field-dependent spin relaxation studies. The preamplifier and the duplexer are completely replaced by new designs that provide low noise figure, large gain and fast recovery. The receiver, the transmitter, and the magnet power supply are modified to operate at low frequency (receiver and transmitter) and at low current (power supply). The performance of the instrument is demonstrated by ²H NMR experiments in the 500 kHz–2 MHz region and is compared to that of instruments based on direct current-superconducting quantum interference device and operated on room-temperature samples. © 2000 American Institute of Physics. [S0034-6748(00)02902-6]

I. INTRODUCTION

While the main direction in the development of nuclear magnetic resonance (NMR) technology is unquestionably towards higher and higher magnetic field strengths, there are some “niche” applications that operate, either by choice or by sheer necessity, at low magnetic fields and at corresponding low resonance frequencies. Low-field magnetic resonance imaging,^{1,2} well logging,^{3,4} nuclear quadrupole resonance detection of explosives,⁵ and controlling food quality by low-field NMR⁶ are examples with the common element of 10⁵–10⁶ Hz resonance frequency. Commercial NMR spectrometers usually cannot explore this frequency range and therefore the potential users must develop their own spectroscopic tools, including all or most electronic components.

The motivation behind this study is also a niche application, frequency-dependent NMR relaxation.^{7–10} This spectroscopic method is a well-developed tool for providing a detailed picture about the microstructure and molecular dynamics in various colloidal systems. There are several techniques to obtain relaxation data in a wide frequency range. The first of those, field cycling,^{11,12} is certainly the one with the widest available range of NMR frequencies. Unfortunately, the technique may severely suffer from some shortcomings,¹³ such as poor field homogeneity (with the corresponding low sensitivity), insufficient temperature and field stability, low reproducibility of relaxation measurements, and low accuracy if the longitudinal relaxation rates approach the ~millisecond region. Moreover, a field-cycling system is far from trivial to build^{14–16} (note that at present there is one commercial source (Stelar, Italy) for field-

cycling instruments). For these reasons, quadrupolar spin relaxation of $I > 1/2$ nuclei such as ²H and ²³Na, has not been frequently explored by field cycling.

On the other hand, quadrupolar spin relaxation of $I > 1/2$ nuclei has proved to be very informative in studying the microstructure and molecular dynamics of various complex fluids, such as micellar solutions, lyotropic liquid crystals, and protein solutions. One frequent advantage of quadrupolar spin relaxation is the relative simplicity of the connected motional correlation functions, which simplifies the analysis of the relaxation data.¹⁷ In the systems mentioned earlier the most significant motional modes that cause the observed spin relaxation are usually described with motional correlation times $\tau_c \sim 10^{-7}$ – 10^{-9} s. Hence, NMR relaxation in the $\omega_0 \sim 100$ kHz–100 MHz region (corresponding to $\omega_0 \sim 1/\tau_c$) holds most of the information. On the other hand, various molecular mechanisms may often lead to relaxation dispersion profiles with rather similar shapes and/or magnitudes. Then, distinguishing among various models leading to the experimentally observed frequency-dependent relaxation rates requires accurate spin relaxation data but in a limited frequency range.¹⁰

While spin relaxation measurements down to a few megahertz are readily available with commercial NMR spectrometers, relaxation measurements at even lower NMR frequencies require home-built instruments with signal-to-noise ratio (SNR) as large as possible and with a good long-time stability.¹⁸ The latter point is important at low frequencies where measurements can take many hours. As concerning the basic electronic setup, one has two choices. First, superconducting quantum interference device (SQUID)-based spectrometers,^{19,20} that were shown to be superior at very low magnetic fields, could be adapted for field-dependent

^{a)}Author to whom correspondence should be addressed; electronic mail: ifuro@physchem.kth.se

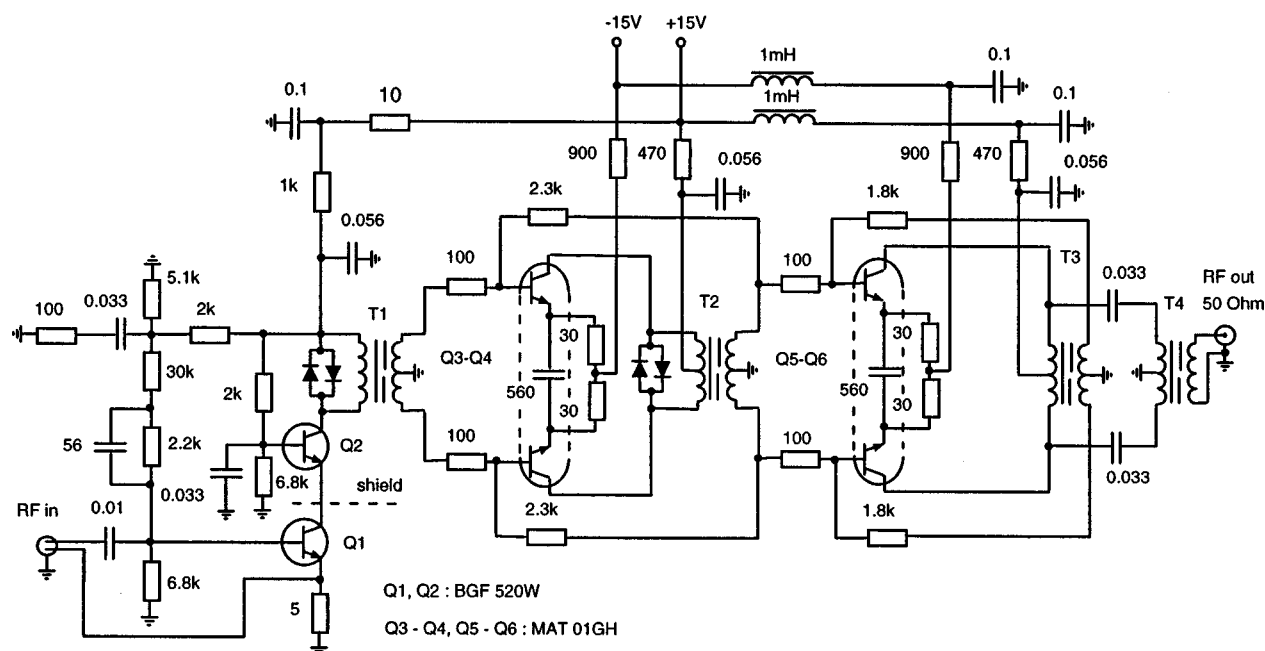


FIG. 1. Detailed schematics of the constructed three-stage rf preamplifier with an operating range of 0.1–5 MHz. The serial tank circuit is connected through a duplexer (Fig. 3) to the first stage based on a cascode arrangement of low-noise bipolar transistors. The second and third stages use balanced differential amplifiers.

relaxation studies. They require, however, a cryogenically cooled pickup coil^{21,22} that, for room-temperature samples, reduces the filling factor (and, correspondingly, the SNR) in the NMR probe. Moreover, it has been shown that over a certain threshold field (for ^2H , around 0.1 T that corresponds to 650 kHz) the SNR in conventional-type NMR spectrometer is larger than that achievable by SQUID-based spectrometers.²⁰

Hence, in many systems, such as in complex fluids, extending the range of a conventional NMR spectrometer might be the best solution to obtain information about molecular structure and dynamics from spin relaxation. (One potential advantage with this solution that more sophisticated pulse programs, mainly used for measuring spin relaxation in anisotropic systems with nonzero static quadrupole splitting,¹⁷ are also readily available at low frequencies.) With many older spectrometers available at low price from second-hand equipment dealers, this is not necessarily an expensive option. On the other hand, the 100 kHz–1 MHz frequency domain imposes technical difficulties since it is at the interface of two rather different regimes, i.e., audio and radio frequency (rf) electronics. In this article, we present our suggestions to overcome these difficulties; the particular spectrometer, that is going to be extended, is a Bruker MSL-90 equipped with an electromagnet. This spectrometer system has already been used for field-dependent relaxation studies^{7,23,24} but only at frequencies ≥ 2 MHz. Most of the points taken up in this study are not vendor specific; in other words, they must be dealt with starting from any type of conventional spectrometers. Partly, we present modifications of some spectrometer parts with limited frequency range. Some of these required changing only some components in the original layout; the corresponding sections are illustrated only by block diagrams. On the other hand, some other parts

had to be replaced completely. For those newly designed parts, such as the preamplifier, the duplexer, and the filters, we provide complete schematics. Additionally, the setup uses a new, commercially available transmitter with some minor modifications. The order of presentation does not follow the sequence in which the presented parts are placed in a spectrometer. Instead, we start with the most involved design and proceed with the less complex ones thereafter.

During the course of this work, previous studies that have dealt with low-frequency spectrometers^{2,4–6} but for other areas of science were found useful. Conversely, we anticipate that some of the points elaborated in this article may help constructing low-frequency NMR spectrometers for various applications.

II. THE PREAMPLIFIER

Most preamplifiers within NMR spectrometers are designed to perform well in the conventional rf frequency range for NMR spectroscopy (10–1000 MHz, depending on spectrometer type). Consequently, they usually are far from optimal performance below 1 MHz. Since any loss of SNR is severely punished in terms of experimental time at low NMR frequencies, one must turn to other alternatives. The easiest option is to use commercially available preamplifiers, different types of which are available from various vendors. Typically, they cover several decades in frequency [direct current (dc)–1 MHz] but we found that they are less suitable for our NMR application. Most seriously, the recovery time after a rf pulse is often very long and, sometimes, the noise factor is higher than desirable. For those reasons, we decided to build a suitable preamplifier (Fig. 1). We attempted to simultaneously achieve (i) high sensitivity and low noise, (ii) a good

broadband performance, and (iii) a fast recovery after a rf pulse. One obvious advantage with a custom-designed amplifier is that it can be fitted best into the NMR probearm; to minimize thermal noise and electromagnetic interference the preamplifier should be built as close to the tank circuit as possible.

The most critical points in designing the first stage is to correctly choose the transistor and the circuit topology. For a gain G_1 of the first stage, the total noise factor F of a preamplifier²⁵ is primarily determined by the noise factor F_1 of the first stage as

$$F = F_1 + \frac{F_2 - 1}{G_1} + \frac{F_3 - 1}{G_2} + \dots, \quad (1)$$

where F_n and G_n are the noise factors and gains of the subsequent stages. Clearly, high G_1 and small F_1 are required. Beside source resistance (which is less controllable), two important contributions to the noise factor F_1 are the intrinsic transistor noise and the noise factor that represents the loss in SNR via the insertion loss of the matching network (due to finite Q of its components, mainly that of the transformer in Fig. 3).

Which transistor is better to use then at the first stage: bipolar or field-effect transistor (FET)? The answer depends on the source resistance. Although one can always transform the source impedance into every optimum noise resistance, a large difference between source and noise resistances may result in a large insertion loss of the matching network. This effect is more pronounced at lower frequencies (in connection to lowering the Q 's of the components). Therefore, one should choose bipolar transistor if the source resistance is low and FET if that is high.²⁶ Such a choice minimizes the noise voltage for a bipolar transistor and the noise current for a FET and, moreover, also minimizes the insertion loss of the matching network. Hence, the choice of transistor depends on the resonance circuit. The original probe architecture of our Bruker MSL spectrometer, that we wanted to preserve, favors a serial arrangement. The 50Ω on-resonance impedance of a serial circuit can be easily matched to the low noise resistance of a bipolar transistor. Therefore, we opted for a BGF 520 W (Philips) that is often used for the rf front end in cellular telephones, radar detectors, etc. (For a parallel resonance circuit a FET is, of course, more feasible. Conversely, FET-based preamplifiers cooled to low temperatures are best to be connected to parallel resonance circuits.)^{27,28}

A large gain G_1 makes the circuit susceptible to oscillations. A high-gain, oscillation-free first stage requires a circuit topology with high reverse isolation: the cascode circuit (Fig. 1) is the most suitable choice and, furthermore, it offers a larger bandwidth than a corresponding common-emitter stage. To avoid coupling between input and output, a good practical construction involves shielding the two transistors from each other as shown in Fig. 1. The input transistor is biased to give a low noise figure when driven by any source resistance from 50 to 200 Ω . The voltage gain of the first stage in Fig. 1 is ≈ 100 .

The noise reduction technique applied in the next two stages of the preamplifier is to use balanced differential am-

plifiers. While such a design is not widespread at high frequencies, it should be superior to conventional preamplifier schemes at low frequencies. However, a large common mode rejection ratio (CMRR) is achieved only with a symmetrical stage accomplished by matched monolithic dual transistors (MAT-01GH, Precision Monolithics Inc.) and accurately balanced loads (see Fig. 1). Two subsequent stages provide double CMRR.

Negative feedback is used to adjust the gain and the bandwidth. The coupling transformers T2 and T3 are inside the feedback loop which makes them linear in the pass band. As another advantage, the large amount of voltage feedback provided by this arrangement allows to extend the low-frequency cutoff. However, the transformers in the feedback loop also increase the risk for oscillations. Hence, a stable operation requires to set the loop gain to a value at which no ripples and peaks are observed in the transfer function of the amplifier. The high-frequency cutoff is determined by the (i) parasitic capacitances and (ii) limitations of the selected ferrite core. To increase the gain at high frequencies, ‘pickup’ capacitors (560 pF) were used between the emitters of the MAT-01GHs.

The most critical point for the frequency response is the construction of the transformer T1 that is not included in the feedback loop. We selected a wideband bifilar transformer with a ferrite core suitable for our frequency range (FT-50J, Amidon Assoc.). The transformer windings of 45 primary and 2×12 secondary provides sufficient impedance to achieve the desired low frequency cutoff. The design in Fig. 1 was measured to provide 0.1–5 MHz (-3 dB points) pass-band. The overall gain of the preamplifier (set to $A_V \approx 5000$) is adequate for most applications²⁹ and it allows us to effectively use the dynamic range of our receiver (see later).

The dead time of the preamplifier depends on the speed of dissipating the energy of the resistive-capacitive (RC) networks after the rf pulse.³⁰ Many commercial preamplifiers, particularly those operated from dc, suffer from this effect for as long as a millisecond. Since our preamplifier is designed for experiments at low frequency, we had to apply large (10–50 nF) values bypass and coupling (to establish true alternating current grounds) capacitors. Those large capacitors, of course, prolong the dead time and therefore their capacitances were kept to as low as possible. To further decrease the dead time (i) crossed diodes were placed across the collector loads of the first two stages³¹ and (ii) the power supply rails were decoupled by low- Q capacitors (not shown in Fig. 1). Finally, a dead time of 5 μ s was achieved which is much shorter than the ringing time of the tank circuit.

Very often the preamplifier noise performance is determined by the ground noise²⁵ and not by the thermal noise of its active components. In such a situation the filters and the grounded shields are ineffective. The two available solutions are to establish a true ground reference point by either lifting the preamplifier ground to the equipment chassis or using a balanced power system²⁵ (see, for example, those of Equi=Tech, Inc.). The first option is cheap and is based on the 5 Ω resistor between the ground and emitter of the first transistor. Because 5 Ω is much larger than the ground impedance between source and preamplifier grounds, it sets the

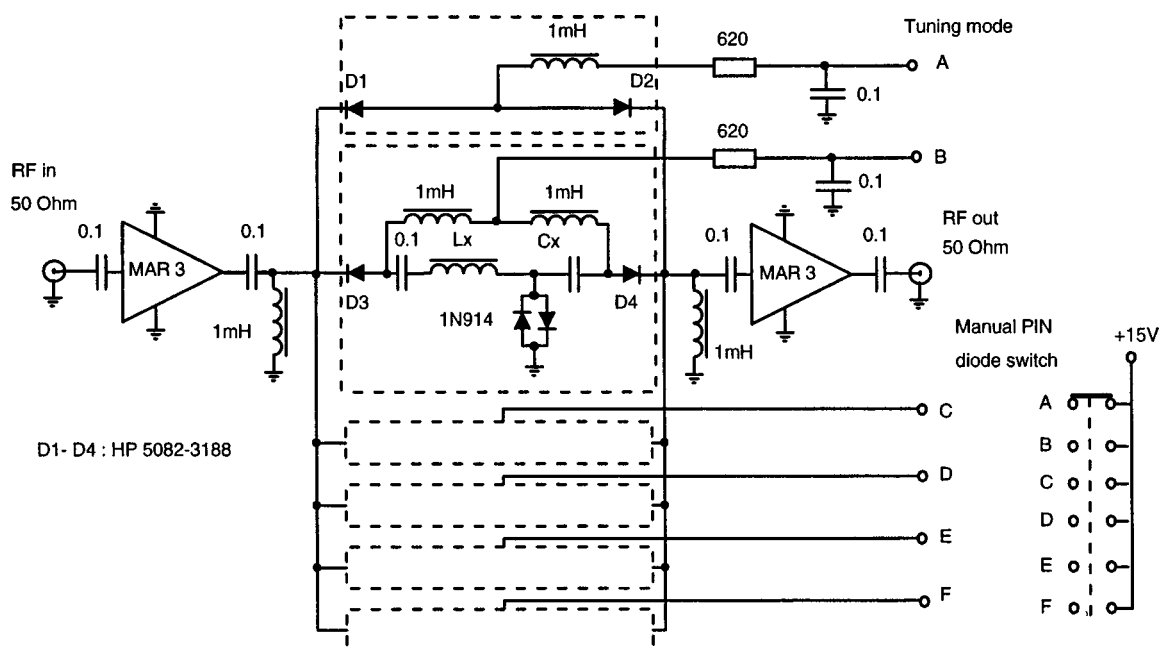


FIG. 2. Detailed schematics of the output filter of the preamplifier. The values of capacitance C_x and inductance L_x were set in the different sets to provide the appropriate central frequencies, see Table I. Different filter sets are selected manually by PIN switches.

potential at the emitter of the first transistor to the ground of the signal source (that is free of ground noise after the transformer of the matching circuit, Fig. 3). Although this is a less effective solution than using balanced power, it has sufficiently reduced our noise floor. Finally, the noise figure of the preamplifier in Fig. 1 has been measured to be ≈ 1.3 dB over the passband.

Signal and noise are amplified together in a bandwidth defined by the filter attached to the preamplifier output. There are two equally valid approaches for the filter design between 100 kHz and 1 MHz, i.e., active and passive filters. Unfortunately, we failed, despite intensive attempts, to construct a suitable active filter with variable central frequency and bandwidth for our target frequency range. Thus, several simple inductive-capacitive (IC) bandpass filters were built instead to cover the range of our resonance frequencies (Fig. 2). Each filter, covering a particular narrow (see Table I) band within the passband of the preamplifier, is activated by positive-intrinsic-negative (PIN) switches (see D1-D4). The filters also protect the receiver from overload³² by cutting the rf amplitude with crossed diodes to the value determined by the L_x/C_x ratio (the higher is the ratio the better is the protection). On the other hand, the insertion loss becomes intolerable for large L_x/C_x ratios. Hence, the L_x/C_x ratio was

optimized for each band (see Table I) so that it allowed to limit the rf amplitude to 10 mV. To provide 50 Ω termination and appropriate gain over the required frequency range, two monolithic amplifiers MAR-3SM (Mini-Circuits) were used at both ends.

III. THE PROBE AND THE DUPLEXER

At low frequencies one has to choose between two suitable probe configurations: single solenoid and quadrature coils. The former requires good electric isolation of the preamplifier input from the transmitter during the rf pulse, which necessarily introduces an insertion loss that can spoil the noise performance of the preamplifier. The latter provides a large (-60 dB, the lower the frequency the better the isolation) natural isolation and requires no additional protection. On the other hand, the quadrature pair of coils in the geometry provided by an electromagnet should involve one solenoid and one saddle coil that either requires extra transmitter power or provides a low signal receptivity. Moreover, fine mechanical tuning is a condition to achieve the desired isolation. For these reasons and for convenience, we chose instead a single solenoid coil with the original 10 mm coil diameter (the optimal diameter is certainly not less than that) and 2.5 cm length. With maximum winding density (0.2 mm copper wire) this choice provides an unloaded $Q = 30$ at 0.5 MHz. Although this coil geometry is less than optimal^{29,33-35} it proved to be sufficient (see Sec. VI).

The probe-receiver interface is a duplexer (Fig. 3) that couples the probe to the receiver and decouples (for protecting the preamplifier) the receiver from the transmitter. The latter function is provided by pairs of crossed Zener-diodes D1-D8 BZX55-2.4 and diodes 1N4441 (additionally, these crossed diodes suppress eventual noise from the transmitter, see later). A usual choice for coupling the probe to the receiver is the $\lambda/4$ -wave network. High isolation, low inser-

TABLE I. The component values and experimental parameters of the LC filter shown in Fig. 2.

Central frequency (MHz)	Bandwidth (kHz)	Insertion loss (dB)	Inductance L_x (μ H)	Capacitance C_x (pF)
0.5	80	-1.6	330	300
0.7	120	-1.5	200	270
1.0	180	-1.0	156	180
1.5	200	-0.9	133	82
2.0	300	-0.8	100	71

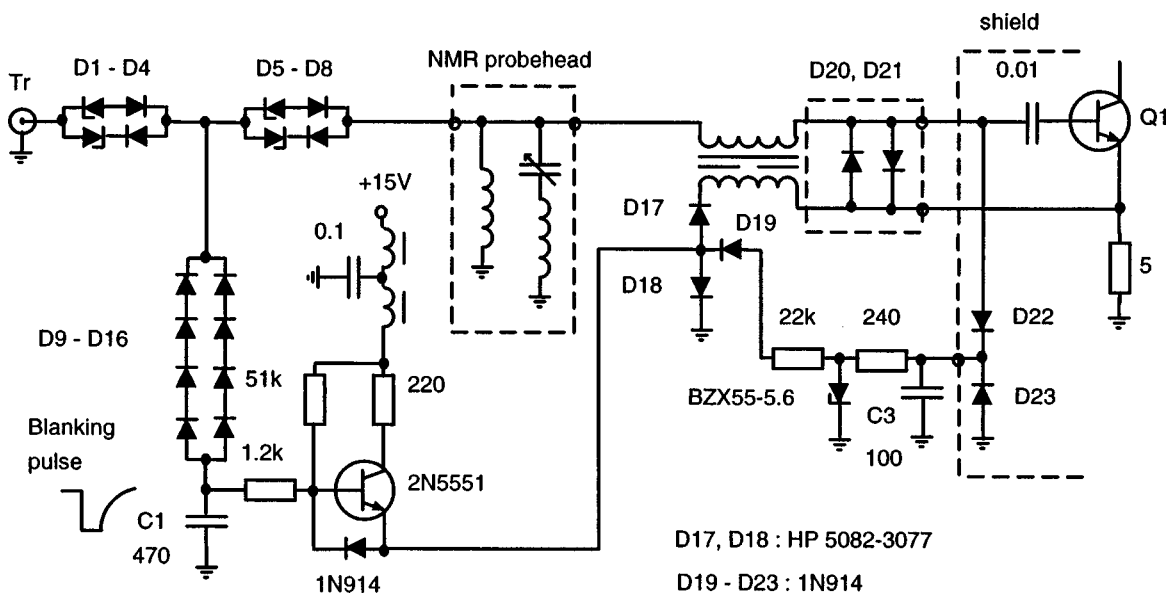


FIG. 3. Detailed schematics of the constructed duplexer. The device protects the preamplifier, suppresses the ringing of the tank circuit, and decouples the ground noise from the preamplifier input.

tion loss, and a good impedance matching require a high- Q network that is difficult to achieve at low frequencies. The selected circuit shown in Fig. 3 has been customized after Engle³⁶ and, in addition to a low insertion loss (0.6 dB) and a high isolation (36 dB), it offers a broadband response.

During the receive time a current of about 17 mA biases the PIN diodes D17-18 "on" which short cuts the secondary winding of the transformer and presents a low-impedance path for the signal. (Note that the depletion voltage of the selected PIN diodes must be much smaller than the voltage arising from the transmitter pulse. In our case the former is 50 V. This requires that the transmitter power is >100 W.) This current value is a compromise between two conflicting effects: increasing the current on the PIN diodes decreases the insertion loss but increases the switching time. The performance of the duplexer depends strongly on the transformer characteristics. The 30 turns bifilar transformer was constructed to have a broad enough passband and was wound on a ferrite toroid with core size suitable for our high rf power (FT-50J, Amidon Assoc.). To any common-mode noise currents the transformer has high impedance and therefore the duplexer possesses an additional feature to suppress the ground noise.

During the transmit time the rf pulse is half-wave rectified and low-pass filtered by four pairs D9-16 of 1N4441 diodes and the capacitor C1. Thus, a blanking pulse is produced (see Fig. 2) that effectively cuts off the transistor 2N5551 and removes the bias from the PIN diodes. As a result, the high impedance of the transformer reduces first the pulse voltage that is then limited to 0.6 V by the crossed diodes. A good isolation requires high inductance of the transformer. Moreover, the blanking pulse has to be well shaped. The time constant of the filter applied after rectifying must be long enough to keep the gating pulse smooth while it has to be short enough (less than 300 ns that is the rise time of the rf pulse at the highest operation frequency for this duplexer which is 5 MHz) to switch on the blanking suffi-

ciently quick. Moreover, the time constant also sets the amplitude of the gating pulse high enough to provide 50 V reverse bias for the particular diodes at which those are fully depleted. The power loss of the transmitter was less than 1 dB at 600 W rf pulse power and the shape of the rf pulse is unchanged by the duplexer. The minimum and average isolations in the blanked mode are 32 and 36 dB, respectively, in the 100 kHz–5 MHz band.

The ringdown of the tank circuit can be excessively long at low frequencies. There are two regimes to distinguish.³⁰ The first one is immediately after the rf pulse when the crossed diodes D1-D8 conduct and the final stage of the transmitter is already blanked off. The time constant of the ringing in this regime is entirely determined by the unloaded Q of the tank circuit. The second ringing mode when crossed diodes D20-D21 conduct is much longer than the first one and thus requires particular attention. This ringing is best reduced by an active Q spoiler³⁰ that drains off ringing at the front stage of the preamplifier. For convenience, the circuit D22-D23 is activated by essentially the same pulse as used for gating the duplexer (except that its "softness" can be varied by capacitor C3 to avoid extra ringing caused by the blanking pulse itself). The ringdown time we achieved with this unit is less than 30 μ s at 500 kHz (see Fig. 4).

Sweep-frequency measurement of the duplexer with 50 Ω termination estimates the insertion loss to less than 1 dB from 100 kHz to 5 MHz with 17 mA of bias applied to each diode. This rather large forward bias provides a very low (not measurable) harmonic distortion in the NMR signal. The contribution of PIN diodes to the preamplifier noise is negligible.

IV. THE RECEIVER AND THE TRANSMITTER

Although it would perhaps be relatively easy to build a separate digital receiver (that is truly frequency independent) for our low-frequency range, we did not consider this as an

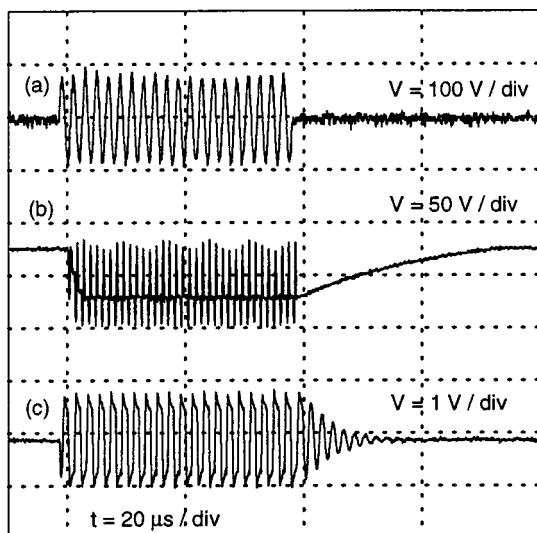


FIG. 4. The rf input pulse (a), the gating pulse (b) at the duplexer in Fig. 2. Figure (c) has been obtained at the preamplifier output and therefore the decay provides the total recovery characteristics of the system at 500 kHz.

option since we wanted to preserve the compact functionality of the spectrometer. Moreover, the original Bruker MSL receiver is very broadband device (2–400 MHz) that combines good transient response with the highest dynamic range with minimal distortions. It was therefore a realistic goal to expand the operating frequency range down to 0.1 MHz without spoiling the excellent original performance. The part of the receiver, that is responsible for shifting the phase of the reference frequency, operates at the fixed frequency of 70 MHz and is therefore entirely frequency independent. This limits the necessary modifications to the dashed box in Fig. 5 where the some components with strong frequency dependence in the $<2 \text{ MHz}$ region were replaced by frequency-independent ones. First, new double balanced mixers (DBM2 in Fig. 5, SRA-6H, Mini-Circuits) were included instead of the original ones in the quadrature detector. Second, new rf monolithic amplifiers (MAR, Mini-Circuits) replaced the old ones at the ports of these mixers; care has to be taken to

adjust the gain (by fixed resistive attenuators) for supplying a signal with proper level to the rf and local oscillator (LO) ports. It is also important to have a proper wideband 50Ω termination at every port of DBM2 which is provided by the monolithic amplifiers. Without these precautions one obtains nonlinearity, distortions, and extra noise.

Adequate power, blanking capability, and wide frequency range determine the choice of the transmitter. In particular, rapid and complete amplifier blanking is necessary to provide high electrical isolation from rf emission and thermal noise. The necessary power range was defined by having the capacity to excite broad (10–50 kHz) NMR spectra. Hence, we selected a commercially available transmitter (Amplifier Research 250L) that is supposed to deliver 750 W pulse power into a 50Ω load in the frequency range 10 kHz–220 MHz and provides, when blanked, 90 dB isolation. Experimentally, any extra noise originating from the amplifier in the blanked state was smaller than noises appearing from other sources at the preamplifier input. To obtain a good pulse shape, the gating pulse must open the transmitter a few microseconds before the pulse on the rf input; thus, the gating pulse has been supplied by the external trigger lines of the spectrometer which also required the adequate modifications of all the applied pulse programs. Although the amplifier is wideband, blanking it produces some low frequency transients which were suppressed by a home-built high-pass ($>300 \text{ kHz}$) filter.

V. THE POWER SUPPLY OF THE ELECTROMAGNET

Our electromagnet is equipped with a Bruker HS 90-VAR power supply (PS) operating in constant current²⁶ (CC) mode that provides a current and field stability at high magnetic fields better than 10^{-4} . A flux stabilizer and NMR lock system (operating on an auxiliary coil) increases the field stability further by more than two orders of magnitude. However, NMR experiments at low ($<2 \text{ MHz}$) frequencies require low ($\sim 0.1 \text{ T}$) fields even for nuclei with relatively low magnetogyric ratios, such as ^2H , ^{23}Na , and ^{31}P . Such low

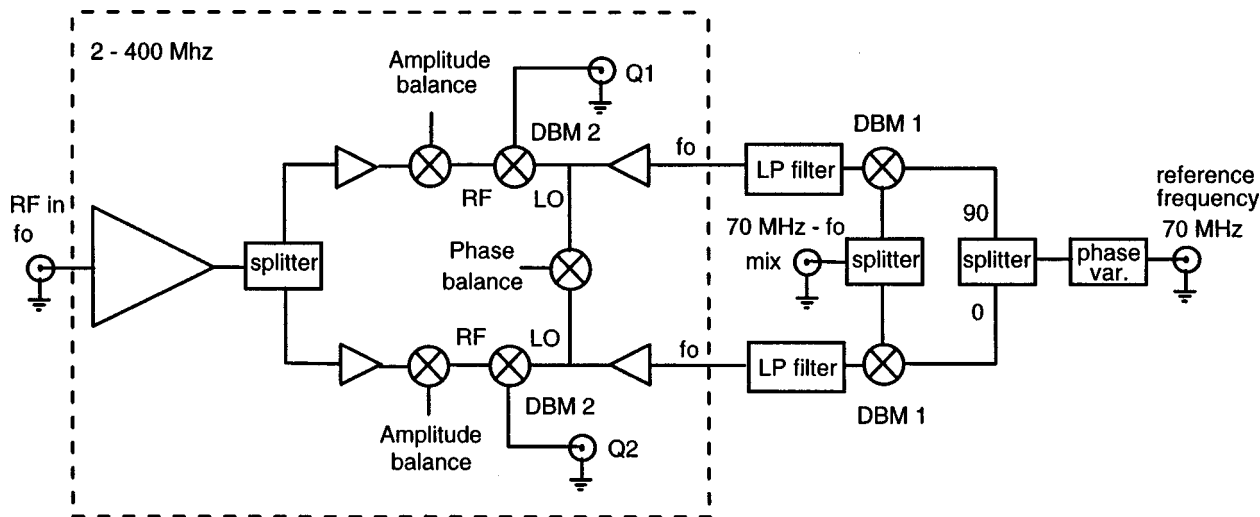


FIG. 5. Block diagram of the receiver of our Bruker MSL spectrometer. Extending its operating range to low ($>0.1 \text{ MHz}$) frequencies was made by replacing frequency-dependent elements in the dashed box with components of appropriate characteristics.

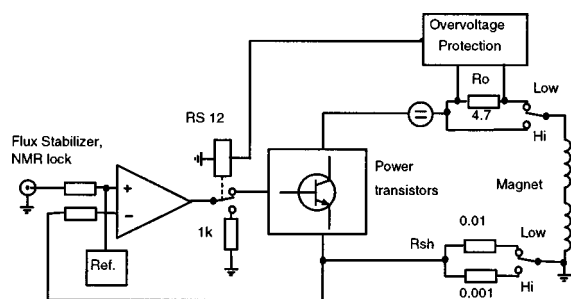


FIG. 6. The block diagram of the PS of the electromagnet (Bruker HS 90-VAR) with the changes to allow operating it in constant current mode at low (<6 A) currents. High power relays switch between the two operating modes.

fields are created by very low (<6 A) currents at which the voltage drop across the power transistors becomes too high. Hence, the current of the PS is not stabilized. This problem can be simply remedied by inserting a high-power resistor R_0 into the current path (see Fig. 6) which decreases the voltage drop on the power transistors and sets them into CC mode even at low currents. The increased value of shunt resistor R_{sh} improves the regulation at low currents. This resistor has a temperature coefficient of 50 ppm to keep the field stable upon heating. With the improved current stability, the flux stabilizer and the NMR lock remain effective down to 0.01 T. Finally, high power relays are used to manually switch between the two current regimes. To prevent damage caused by the current increasing uncontrollably over the rating value for R_0 , a simple protection circuit (based on a voltage sensor that switches a relay, not shown) was also added.

VI. EXPERIMENTAL RESULTS

The performance of the modified spectrometer is demonstrated by ^2H NMR spectra recorded at different frequencies (Fig. 7). The signal was obtained by a single 90° pulse, from which the presented spectra were obtained by Fourier transformation without apodization. At 500 kHz one obtains $\text{SNR}=32$ for the line with a half width of 5.5 Hz. The spectral broadening of about 4.5 Hz is due field inhomogeneity of ≈ 5 ppm. (The best achievable homogeneity in the investigated frequency range is about 2 ppm.) The frequency dependence of the SNR is strong, roughly as expected from theory. The exception is at 500 kHz, where the SNR drops to a lower value than expected from the performance at higher frequencies.

One can compare the SNR to that obtained at low frequencies by dc-SQUID-based devices in room-temperature samples. Of the few experimental examples, the latest and most advanced one^{21,22} provided the estimated single-scan (peak amplitude)-to-[root-mean-square (rms) noise] ratio of about 2 in the ^1H NMR spectrum of 1 cm³ water at 400 kHz.²² To compare that to our result is somewhat complicated by the fact that those spectra are magnitude ones, while our spectra are phase-sensitive absorption spectra. One must take into account the larger linewidth [500 Hz for the magnitude spectra that corresponds to 300 Hz in phase-sensitive linewidth, the SNR scales as $(\text{linewidth})^{-1}$] and bandwidth

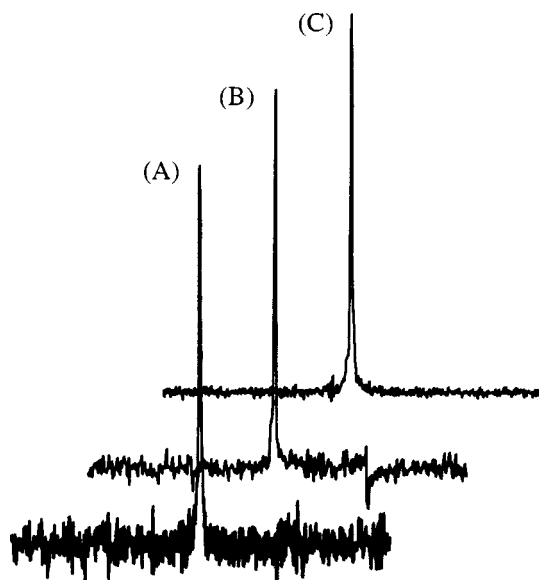


FIG. 7. ^2H NMR spectra of 99% D_2O (≈ 2 cm³ in a 10 mm outer diameter tube) at room temperature recorded by single scans at 0.5 (a), 0.7 (b), and 1.0 MHz (c). The presented spectral window is 900 Hz broad. The SNRs, calculated as signal amplitude divided by the rms noise for 5 kHz filter width, are 32 (a), 100 (b), and 156 (c).

[50 kHz, the SNR scales as $(\text{bandwidth})^{-1/2}$] in that study. Moreover, the relative signal³⁴ (obtained at about the same Larmor frequency) scales as $\gamma I(I+1)$ which is a 2.25 factor when comparing ^1H to ^2H spectra. Finally, our observed SNR must be scaled down to 400 kHz. Thus, one can calculate that at 400 kHz the SQUID SNR is about a factor of two larger than the scaled (from the present data at 500 kHz) SNR of our system. On the other hand, the SNRs of SQUID and our conventional NMR system are roughly the same at 700 kHz. This fits well to the theory²⁰ that expects the cross-over between SQUID-based and conventional SNRs at around this frequency for ^2H .

The application of the frequency-extended spectrometer to frequency-dependent spin relaxation studies is demonstrated in Figs. 8 and 9. The sample is a micellar solution (28.8 wt %) of decylammonium chloride in water (deuterium

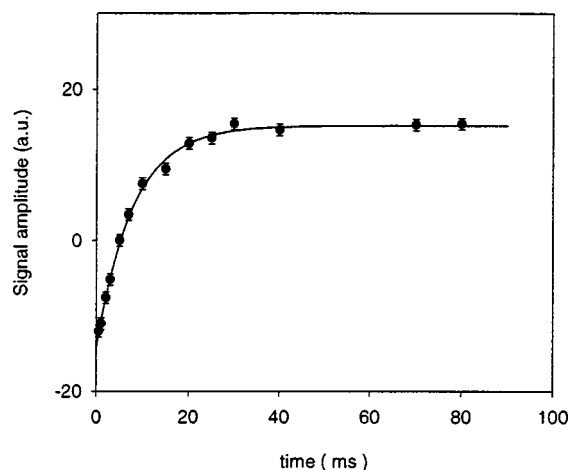


FIG. 8. The result of a ^2H inversion recovery experiment performed at 0.5 MHz in a 28 wt % micellar solution of selectively deuterated decylammonium chloride at 55 °C.

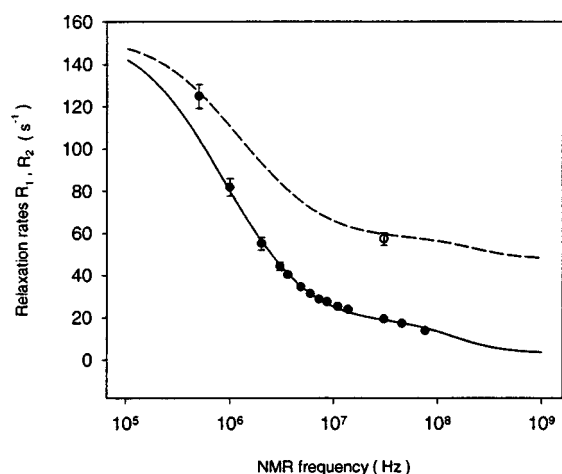


FIG. 9. The frequency dependence of the ^2H longitudinal relaxation rate of selectively deuterated decylammonium chloride in a 28 wt % micellar solution at 55°C (see Ref. 37). One high-frequency transverse relaxation rate (open symbol) is given as well. The continuous and dashed lines are fits within the frame of a motional model that does not account for the collective reorientation of the micellar aggregates in this concentrated solution.

depleted), with the surfactant selectively deuterated at its α -methylene group.³⁷ Figure 8 presents a relaxation curve obtained from the inversion recovery experiment on ^2H at 55°C and at 500 kHz. (16 000 scans with 12 h experimental time). The obtained longitudinal relaxation rate $R_1 = 126\text{ s}^{-1}$ has an estimated 2σ error of $\pm 4.5\%$. This accuracy is sufficient to show (Fig. 9) that a theoretical model that does not take account of the collective reorientation of micelles in a concentrated solution does not fit to experimental data.³⁷ Note that this discrepancy would not have been observed if only NMR frequencies ≥ 2 MHz were available.

VII. DISCUSSION

This work shows how to expand the frequency range of conventional NMR spectrometers to the 10^5 Hz range. The various replacements and modifications presented here provide a frequency range down to 100 kHz. The spectrometer part that currently limits us to 500 kHz is the original pulse modulator of the Bruker MSL-90 that provides too low pulse output below 500 kHz. If necessary, this problem can be easily solved. (Note that the 300 kHz limit of the high-pass filter at the transmitter output was only a choice of convenience.) On the other hand, as demonstrated by Fig. 7 and by the comparison to the SQUID results,²² going much below 500 kHz is, in any case, rather impractical with conventional NMR technology. If necessary, this drawback could be partly compensated in the 100–500 kHz region by a coil of larger diameter and a corresponding larger sample volume.

If SQUID-based solutions are not desirable (such as in our temperature-sensitive samples) this low-frequency limit leaves only a small gap between conventional spin relaxation experiments (≥ 500 kHz) and “ $T_{1\rho}$ ”-type techniques (< 100 kHz). Assuming that the well-known shortcomings of $T_{1\rho}$ -type experiments, most importantly excessive sample heating, could be cured this development opens an alternative strategy to wide-range relaxation dispersion studies without field cycling.

ACKNOWLEDGMENT

This work has been supported by the Swedish Natural Science Research Council (NFR). Sergey Dvinskikh and Pavel Yushmanov are thanked for their help during the construction.

- ¹L. Kaufman, D. Kramer, J. Carlson, and M. Arakawa, in *Encyclopedia of Nuclear Magnetic Resonance*, edited by D. M. Grant and R. K. Harris (Wiley, Chichester, 1996), Vol. 5, p. 2852.
- ²B. T. Saam and M. S. Conradi, *J. Magn. Reson.* **134**, 67 (1998).
- ³R. L. Kleinberg, in *Encyclopedia of Nuclear Magnetic Resonance*, edited by D. M. Grant and R. K. Harris (Wiley, Chichester, 1996), Vol. 8, p. 4960.
- ⁴D. D. Griffin, R. L. Kleinberg, and M. Fukuhara, *Meas. Sci. Technol.* **4**, 968 (1993).
- ⁵T. N. Rudakov, A. V. Belyakov, and V. T. Mikhaltsevich, *Meas. Sci. Technol.* **8**, 444 (1997).
- ⁶F. Capozzi, M. A. Cremonini, C. Luchinat, G. Placucci, and C. Vignali, *J. Magn. Reson.* **138**, 277 (1999).
- ⁷O. Söderman, U. Henriksson, and U. Olsson, *J. Phys. Chem.* **91**, 116 (1987).
- ⁸V. P. Denisov, J. Peters, H. D. Hörlein, and B. Halle, *Nature Struct. Biol.* **3**, 505 (1996).
- ⁹V. P. Denisov, K. Venu, J. Peters, H. D. Hörlein, and B. Halle, *J. Phys. Chem. B* **101**, 9380 (1997).
- ¹⁰I. Furó and B. Halle, *Phys. Rev. E* **51**, 466 (1995).
- ¹¹F. Noack, *Prog. Nucl. Magn. Reson. Spectrosc.* **18**, 171 (1986).
- ¹²F. Noack, S. Becker, and J. Struppe, *Annu. Rep. NMR Spectrosc.* **33**, 1 (1997).
- ¹³E. Anoardo and D. J. Pusiol, *Phys. Rev. Lett.* **76**, 3983 (1996).
- ¹⁴G. Schauer, W. Nusser, M. Blanz, and R. Kimmich, *J. Phys. E* **20**, 43 (1987).
- ¹⁵M. Blanz, T. J. Rayner, and J. A. S. Smith, *Meas. Sci. Technol.* **4**, 48 (1993).
- ¹⁶C. Job, J. Zajicek, and M. F. Brown, *Rev. Sci. Instrum.* **67**, 2113 (1996).
- ¹⁷B. Halle, P. O. Quist, and I. Furó, *Liq. Cryst.* **14**, 227 (1993).
- ¹⁸R. Sitnikov, I. Furó, and U. Henriksson, *J. Magn. Reson., Ser. A* **122**, 76 (1996).
- ¹⁹C. Connor, *Adv. Magn. Opt. Reson.* **15**, 201 (1990).
- ²⁰Y. S. Greenberg, *Rev. Mod. Phys.* **70**, 175 (1998).
- ²¹S. Kumar, B. D. Thorson, and W. F. Avrin, *J. Magn. Reson., Ser. B* **107**, 252 (1995).
- ²²S. Kumar, W. F. Avrin, and B. R. Whitecotton, *IEEE Trans. Magn.* **32**, 5261 (1996).
- ²³O. Söderman, H. Walderhaug, U. Henriksson, and P. Stilbs, *J. Phys. Chem.* **89**, 3693 (1985).
- ²⁴M. Törnblom and U. Henriksson, *J. Phys. Chem.* **101**, 6028 (1997).
- ²⁵H. W. Ott, *Noise Reduction Techniques in Electronic Systems* (Wiley, New York, 1988).
- ²⁶P. Horowitz and W. Hill, *The Art of Electronics* (Cambridge University Press, Cambridge, 1989).
- ²⁷P. Styles *et al.*, *J. Magn. Reson.* **60**, 397 (1984).
- ²⁸M. Jerosch-Herold and R. K. Kirschman, *J. Magn. Reson.* **85**, 141 (1989).
- ²⁹D. I. Hoult, *Prog. Nucl. Magn. Reson. Spectrosc.* **12**, 41 (1978).
- ³⁰E. Fukushima and S. B. W. Roeder, *Experimental Pulse NMR* (Addison-Wesley, Reading, 1981).
- ³¹J. D. Ellett *et al.*, *Adv. Magn. Reson.* **5**, 117 (1971).
- ³²H. T. Stokes, *Rev. Sci. Instrum.* **49**, 1011 (1978).
- ³³D. I. Hoult and R. E. Richards, *Proc. R. Soc. London, Ser. A* **344**, 311 (1975).
- ³⁴D. I. Hoult and R. E. Richards, *J. Magn. Reson.* **24**, 71 (1976).
- ³⁵D. I. Hoult and P. C. Lauterbur, *J. Magn. Reson.* **34**, 425 (1979).
- ³⁶J. L. Engle, *Rev. Sci. Instrum.* **49**, 1356 (1978).
- ³⁷M. Törnblom, R. Sitnikov, and U. Henriksson, *J. Phys. Chem. B* (in press).